

# Nickel oxide nanoparticles induced DNA damages in human liver cells

Mahmoud Abudayyak<sup>1,2</sup> , E. Elif Güzel<sup>3</sup> , Gül Özhan<sup>1</sup> 

<sup>1</sup>Istanbul University, Faculty of Pharmacy, Department of Pharmaceutical Toxicology, Istanbul, Turkey

<sup>2</sup>Karadeniz Technical University, Faculty of Pharmacy, Department of Pharmaceutical Toxicology, Trabzon, Turkey

<sup>3</sup>Istanbul University - Cerrahpasa, Cerrahpasa Medical Faculty, Department of Histology and Embryology, Istanbul, Turkey

**ORCID IDs of the authors:** M.A.0000-0003-2286-4777; E.E.G.0000-0001-9072-3322; G.Ö.0000-0002-6926-5723

**Cite this article as:** Abudayyak, M., Guzel, E. E., & Ozhan, G. (2021). Nickel oxide nanoparticles induced DNA damages in human liver cells. *Istanbul Journal of Pharmacy*, 51(2), 175-182.

## ABSTRACT

**Background and Aims:** Nickel oxide nanoparticles (NiO-NPs) are one of the most used nanoparticles, especially as photosensitizers. Although some studies evaluate their toxicity in the liver, the information about their toxicity at the cellular and molecular levels is still controversial. In the present study, it was aimed to investigate the *in vitro* toxic potentials of NiO-NPs (average size 15.0 nm) in the liver (HepG2) cell line.

**Methods:** NiO-NPs were characterized by Transmission Electron Microscopy (TEM), the cellular uptake of NPs and the morphologic changes were evaluated by TEM and Inductively Coupled Plasma-Mass Spectrometry (ICP-MS), the cytotoxicity was evaluated by MTT and neutral red uptake (NRU) tests, comet assay was used for genotoxicity, Annexin V-FITC/propidium iodide (PI) apoptosis detection kit was used for apoptosis/ necrosis evaluation and Enzyme-Linked Immune Sorbent Assays (ELISA) kits were used for the potential of oxidative damage.

**Results:** Our results showed that cellular uptake of NiO-NPs led to morphological changes in the cells, and caused cell death (IC<sub>50</sub> was 146.7 µg/mL by MTT) mainly by apoptosis. Genotoxicity and oxidative damage were observed to be in a dose-dependent manner.

**Conclusion:** Results confirm previous data and draw attention to the toxic effects of NiO-NPs; further *in vivo* and *in vitro* studies need to be done to clarify the safety or toxicity of NiO-NPs.

**Keywords:** Nickel oxide, Nanoparticles, Genotoxicity, Oxidative stress, Apoptosis

## INTRODUCTION

Humans are exposed to NPs through dermal absorption, ingestion, and inhalation due to their wide range of applications (Ahamed, Ali, Alhadlaq, & Akhtar, 2013; Ahmad, et al., 2013; Kim, Yu, Park, & Yang, 2010). In addition to direct exposure, indirect exposure to NPs is possible *via* the content in bulk material (Dhawan & Sharma, 2010). Studies have shown that NPs are more toxic than their bulk forms; different toxic effects like cytotoxicity, genotoxicity, oxidative damage and morphological changes in the exposed organ were observed after exposure to NPs (Oberdorster, 2001; Zhang, et al., 2012). However, the

information concerning NPs' effects on humans and the environment systems are still insufficient (Arora, Rajwade, & Pankar, 2012; Barillet et al., 2010; Brooking, Davis, & Illum, 2001; Chen et al., 2015). Different factors, such as the properties of NPs including the particles size, shape and surface charges, the route of exposure, the exposed cells' sensitivity and the assays used play an important role in the toxicity that will emerge and the results that will be obtained (Boverhof & David, 2010; Horev-Azaria et al., 2011; Horie et al., 2009; Napierska, Thomasen, Lison, Marten, & Hoet, 2010; Oberdorster, Oberdorster, & Oberdorster, 2005; Schrand et al., 2010).

## Address for Correspondence:

Gül ÖZHAN, e-mail: gulozhn@istanbul.edu.tr

Submitted: 08.12.2020

Revision Requested: 05.04.2021

Last Revision Received: 07.04.2021

Accepted: 16.04.2021

This work is licensed under a Creative Commons Attribution 4.0 International License.



NiO-NPs are widely used as catalysts, pigments, and sensors in different medical and industrial applications because of their superior properties (Capasso, Marina, & Maurizio, 2014; Horie et al., 2009; Morimoto et al., 2011; Schrand et al., 2010). According to the International Agency for Research on Cancer (IARC), NiO and other Ni compounds have been classified as carcinogenic to humans (Group 1) (IARC, 1990; Dunnick et al., 1988). Additionally, the solubility of NiO-NPs is assumed to be higher than the fine particles, and so, it is thought that NiO-NPs release more Ni<sup>2+</sup> than fine particles leading to more toxic effects (Horie et al., 2011). Researches have mainly focused on their pulmonary toxicity, and reported that Ni-based NPs induced oxidative stress and inflammatory responses in the respiratory system (Ahamed et al., 2013; Capasso, Marina, & Maurizio, 2014; Cho et al., 2010; Horie et al., 2011; Kang et al., 2011; Morimoto et al., 2011; Morimoto et al., 2010; Nishi et al., 2009; Ogami et al., 2009; Oyabu et al., 2007; Siddiqui et al., 2012). Additionally, it is well known that NiO-NPs are absorbed through the intestines and distributed with the blood to different organs like the liver; there are few controversial reports about NiO-NPs' toxic potential in the liver (Ahmad et al., 2013; Oberdorster, Oberdorster, & Oberdorster, 2005; Siddiqui et al., 2012).

In the present study, it was aimed to investigate the *in vitro* toxic effects of NiO-NPs on the liver (HepG2 hepatocarcinoma cell). Therefore, the NPs' size was characterized, and the cellular uptake and the cellular morphological changes were evaluated. Cytotoxicity, DNA damage, oxidative stress, and apoptosis were also studied using by *in vitro* methods. The preferred cell line and assays are widely used for NP toxicity studies. Many investigators select the highly differentiated human liver cell lines (HepG2) to study the apical uptake, metabolism, and absorption of nutrients and drugs, etc., as models in *in vitro* conditions (Brand, Hannah, Mueller, Cetin, & Hamel, 2000; Martin, Failla, & Smith, 1997). O'Brien et al., (2006) observed the sensitivity of the cytotoxicity assay was 85% with a specificity of 98% when HepG2 cells were used as an *in vitro* model to predict the hepatotoxic potential of 243 drugs and chemicals.

## MATERIALS AND METHODS

### Chemicals

NiO-NPs, MTT (3-[4,5-dimethylthiazol-2-yl]-2,5-diphenyl-tetrazolium bromide), and neutral red dye were obtained from Sigma (MO, USA). Cell culture mediums, antibiotic solutions, fetal bovine serum (FBS), and phosphate buffer saline (PBS) were purchased from Multicell Wisent (Quebec, Canada). Oxidative stress detection ELISA kits (GSH, 8-OHdG, MDA and PC) were purchased from Yehua Biological Technology (Shanghai, China). Protein detection kits were obtained from Bio-rad (Munich, Germany); Annexin V-FITC/ PI apoptosis detection kits were obtained from Biolegend (CA, USA). The other chemicals were obtained from Merck (NJ, USA).

### Particle size characterization

Dynamic light scattering (DLS) (ZetaSizer Nano-ZS, Malvern Instruments, Malvern, UK) was used to evaluate the average hydrodynamic size of NiO-NPs in the complete cell culture medium. Besides that, TEM (JEM-2100 HR, JEOL, USA) was used to estimate the size and distribution of NiO-NPs according to the

method used by Abudayyak et al., (Abudayyak, Guzel, & Özhan, 2017; 2017b).

### Cell cultures and exposure conditions

HepG2 human hepatocarcinoma cell line (HB-8065; American Type Culture Collection (ATCC), MD, USA) was used in this study. The cells were incubated at 37°C, 5% CO<sub>2</sub> and 90% humidity conditions, in a cell culture medium (Eagle's Minimum Essential Medium, EMEM) supplemented with FBS (10%), and antibiotics (100 units/mL of penicillin, 100 µg/mL of streptomycin). For cell death assays, the cell densities were 1x10<sup>4</sup> cells/mL, for DNA damage evaluation (Comet assay) 1x10<sup>5</sup> cells/mL, and 1x10<sup>7</sup> cells/mL for both uptake by ICP-MS and morphology examinations by TEM. For apoptosis/necrosis and oxidative stress assays, the cell densities were adjusted to 1x10<sup>6</sup> cells/mL.

The particle suspensions were freshly prepared before exposure. Therefore, 1 mg/mL NiO-NPs were suspended in 1 mL complete cell culture medium (containing 10% FBS) and sonicated at room temperature for 15 min and the different exposure suspensions were prepared by diluting with complete cell culture medium.

The cells were treated with different concentrations for 24 h (Abudayyak et al., 2017; 2017b). For the cytotoxicity assays the exposure concentrations were 50-500 µg/mL, for genotoxicity the concentrations were 15-120 µg/mL, and 100-700 µg/mL in the apoptosis/necrosis assay, for oxidative damage assays the exposure concentrations were 50-150 µg/mL, in the cellular uptake assay by ICP-MS (Thermo Elemental X series 2, USA) the concentrations were 50 and 100 µg/mL and they were 50 and 150 µg/mL in the morphology examination and cellular uptake by TEM. The exposure time of the particle suspensions was 24 h.

### Cellular uptake by ICP-MS

The exposed cells were washed twice with the cell culture medium, trypsinized and counted by Luna cell counter (Virginia, USA). The cells were digested by 6 M for 2 h at room temperature and then stored at -20°C until analysis for Ni amount with ICP-MS. The unexposed cells were accepted as the negative control. The test was repeated four times.

### Cellular uptake and morphology by TEM

Glutaraldehyde (2.5%) in Millonig's sodium phosphate buffer (pH 7.4) was used to fix the cells. The cells were centrifuged at 1200 rpm for 10 min, the pellets were washed in Millonig's buffer and centrifuged at 1200 rpm for 10 min. As post-fixation, 1% osmium tetroxide in Millonig's buffer (for 30 min, at room temperature) was used. Before embedding in araldite, agarose gel (2%) was used to block the fixed-cells, and a graded series of ethanol from 30% to absolute (96%) ethanol were used for dehydration. Toluidine blue was used in staining the semi-thin sections of the polymerized blocks, while an ultramicrotome (Reichert UM 3, Austria) was used in the preparation of the ultra-thin sections (50-60 nm). After that, the ultra-thin sections were placed on copper grids; uranyl acetate with lead citrate was used as the stain in this step. TEM (Jeol-1011, Tokyo, Japan) with an accelerating voltage of 80 kV and an attached digital camera (Olympus-Veleta TEM Camera, Tokyo, Japan) was used in photographing and the analysis of the cells.

### Cytotoxicity assays

MTT and NRU assays were used to evaluate the cytotoxic effects of NiO-NPs (Repetto, del Peso, & Zurita, 2008; Van Meerloo, Kaspers, & Cloos, 2011). Therefore, cells ( $1 \times 10^4$  cells/well) were treated with freshly prepared NiO-NP suspension at concentrations of up to 500  $\mu\text{g}/\text{mL}$  (Abudayyak et al., 2017; 2017b). The optical densities (ODs) were read using a microplate spectrophotometer system (Epoch, Germany). The unexposed (negative control) cells were used in the calculation of the half-maximal inhibitory concentration ( $\text{IC}_{50}$ ) values.

### Genotoxicity assay

Comet assay was used in the determination of the genotoxic potential of the NiO-NPs. The unexposed cells were evaluated as the negative control group, while the cells treated with Hydrogen peroxide ( $\text{H}_2\text{O}_2$ ) (100  $\mu\text{M}$ ) were accepted as positive controls. A fluorescent microscope (Olympus BX53, Olympus, Tokyo, Japan) and automated image analysis system were used in scoring the DNA breaks. At least 100 cells were evaluated for each sample, and the tail intensity (percentage of DNA in the comet tail) was used to investigate the DNA damage in the individual cells (Collins, 2004; Speit & Hartmann, 1999).

### Oxidative damage assays

Human GSH, MDA, 8-OHdG, or PC ELISA kits were used to evaluate the oxidative damage in the cells exposed to NiO-NPs, while the Bradford method (1976) was used to measure the protein amount in  $10^6$  cells. ELISA Kits, which are based on biotin double antibody sandwich technology, were used according to the manufacturer's instructions (Abudayyak et al., 2017). A standard calibration curve was used in the calculation of GSH, MDA, 8-OHdG, and PC results, expressed as  $\mu\text{mol}$ ,  $\mu\text{mol}$ ,  $\mu\text{g}$ , and  $\mu\text{g}$  per g protein, respectively.

### Apoptosis assay

Annexin V-FITC with PI apoptosis-necrosis detection kit was used to estimate the apoptotic/ necrotic effects of NiO-NPs. Therefore, the cells were treated with different final concentrations of NPs equivalent to 25, 50, and 75% cell death, respectively. The exposure concentration ranges were 100-200  $\mu\text{g}/\text{mL}$ . The unexposed cells were accepted as a negative control. The cells were washed, collected and adjusted to be  $10^6$  cells in 1 mL. Five  $\mu\text{L}$  of Annexin V-FITC and 10  $\mu\text{L}$  of PI were added to the cells and incubated for 15 min in the dark, at room temperature. The stained cells were spread on microscopic slides and counted under a phase-contrast fluorescent microscope (Olympus BX53, Olympus, Tokyo, Japan). The percent of viable (non-fluorescent), apoptotic (green-fluorescent), and necrotic (red-fluorescent) cells were calculated.

### Statistical analysis

The cytotoxicity assays were done in triplicate and repeated four times while genotoxicity, oxidative stress, and apoptosis assays were done in triplicate and each assay was repeated twice. Data were expressed as mean  $\pm$  standard deviation (SD). The significance of differences between the unexposed and exposed with NPs cells was calculated by one-way ANOVA Dunnett t-test using SPSS version 23 for Windows (SPSS Inc., Chicago, IL). *p* values of less than 0.05 were selected as the levels of significance.

## RESULTS

### Particle size and size distribution

The particle size and size distribution of NiO-NPs were analyzed with TEM images (Figures 1, and 2). In the water, the size of particles ranged from 4.2 to 38.1 nm (average 15.0 nm) with a narrow size distribution. A slight agglomeration/aggregation were noticed after the suspension of NPs in the cell culture medium (Figure 3), the NP sizes ranged from 7.2 to 60.5 nm with an average size of about 21.4 nm. The adsorption of proteins in the NP surfaces and the formation of protein-corona complexes could explain this increase in the size of NPs among water and medium suspensions (Walczyk, Bombelli, Monopoli, Lynch, & Dawson, 2010).

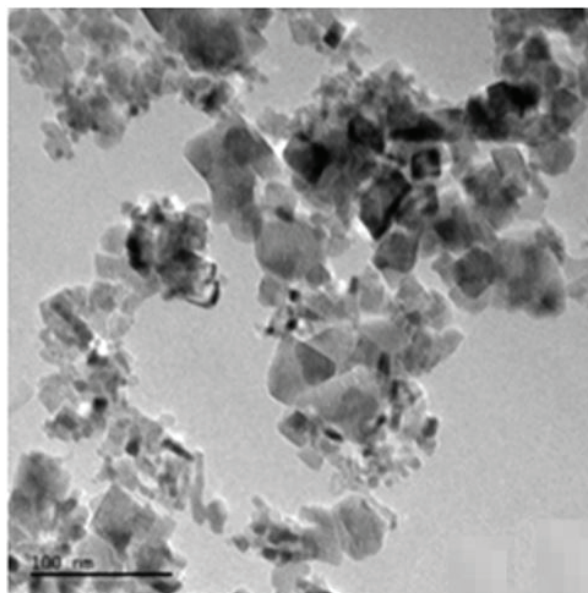


Figure 1. TEM images of NiO-NPs in water.

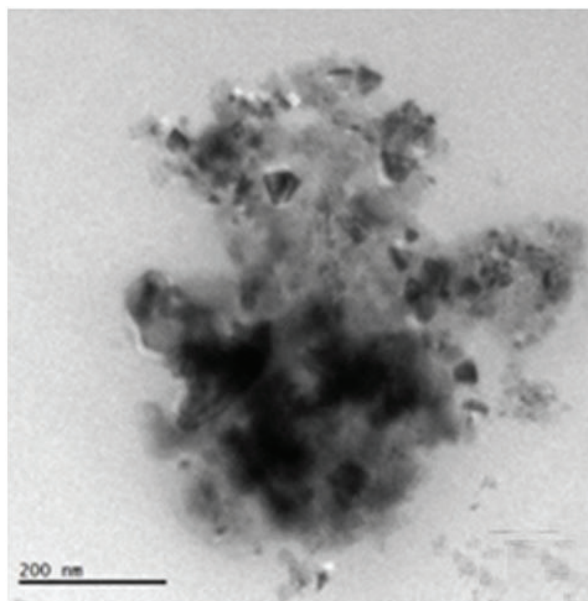
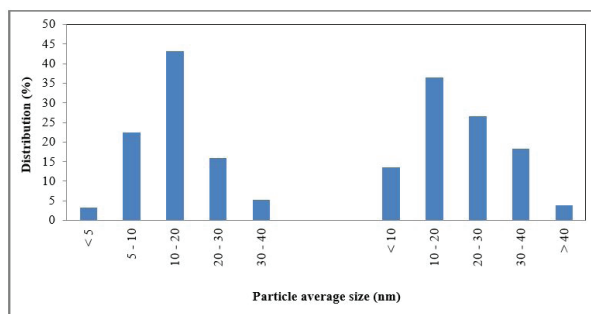


Figure 2. TEM images of NiO-NPs in cell culture medium.



**Figure 3.** TEM images and the size distributions of NiO-NPs in water (a) and cell culture medium (b).

### Cellular uptake

The results of ICP-MS indicate the cellular uptake of NPs after exposure to 50 and 100  $\mu\text{g}/\text{mL}$  for 24 h (Table 1). The cellular uptake of NPs ranged from 1.87 to 7.92  $\text{mg}/10^5$  cells. The inclination of NPs to agglomerate and aggregate at the high concentrations could explain the decrease observed in the cellular uptake at higher exposure-concentration.

	Exposure concentration ( $\mu\text{g}/\text{mL}/10^5$ cells)	Ni amount ( $\text{mg}/10^5$ cells)
<b>HepG2</b>	Negative control	0.02 $\pm$ 0.01
	50	7.92 $\pm$ 0.26
	100	1.87 $\pm$ 0.14

The cells were exposed to 50 and 100  $\text{mg}/\text{mL}$  of NiO-NPs for 24 h. At the end of exposure time, their cellular uptake potentials were determined by ICP-MS, as described in the Methods section. Ni content of the unexposed cells (negative control) and the exposed cells were measured. The assay was repeated four times. The results were presented as mean  $\pm$ SD.

### Cellular morphology

Cellular morphological changes in the cells exposed to NiO-NPs at 50 and 150  $\mu\text{g}/\text{mL}$  were evaluated using TEM photographs and compared to the morphology of the unexposed cells (negative control) (Figures 4-6). The NPs were observed in the cytoplasmic vacuoles of HepG2 cells at both 50 and 150  $\mu\text{g}/\text{mL}$ . The size of the vacuoles was notably large, and particle agglomeration and aggregation within them were prominent at 50  $\mu\text{g}/\text{mL}$ . The cytoplasmic vacuoles were observed to contain myelin figures as well as the NPs. The electron-lucent cytoplasmic vacuoles causing a complete degradation of the cytoplasm, and organelles were not evident. The nuclear and plasma membranes were intact. Although the size of the vacuoles and the NP amount within them were decreased in the cells exposed to 150  $\mu\text{g}/\text{mL}$  of NiO-NPs, cellular damage was greater than with 50  $\mu\text{g}/\text{mL}$  of NiO-NPs. In subjective assessment, according to the morphological changes in the cells including cytoskeleton, organelle shape, and size, *etc.*, almost half of the cells were assessed as apoptotic or necrotic (Figures 4-6).

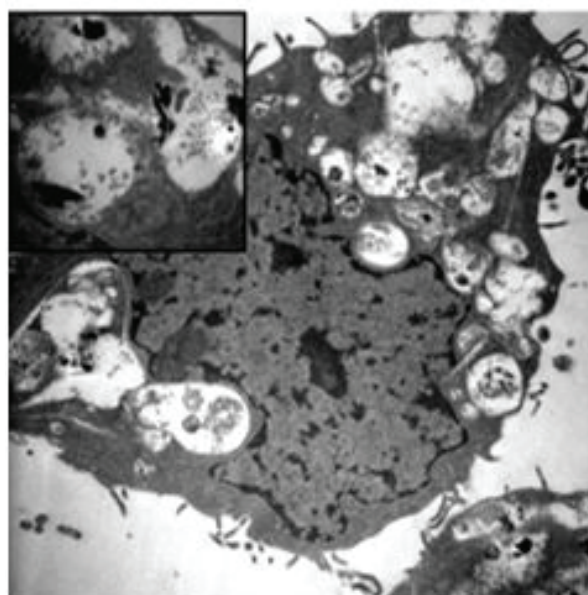


**Figure 4.** TEM observations of HepG2 cells after exposure to NiO-NPs for 24 h.

HepG2 cells exposed to NiO-NPs at 50  $\mu\text{g}/\text{mL}$

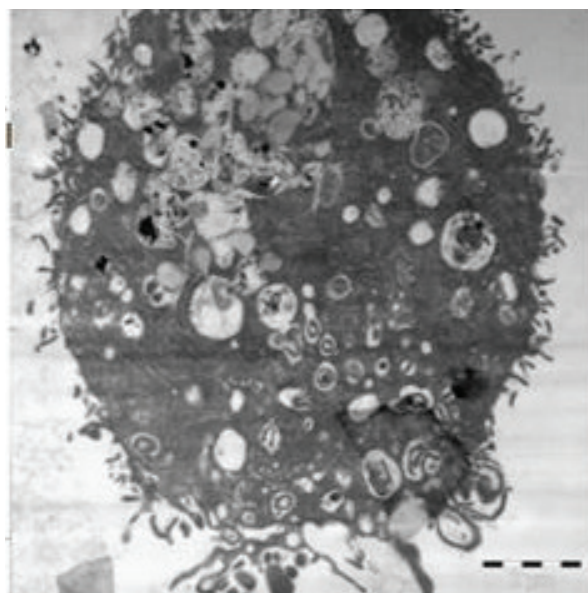


**Figure 5.** TEM observations of HepG2 cells after exposure to NiO-NPs for 24 h.

HepG2 cells exposed to NiO-NPs at 100  $\mu\text{g}/\text{mL}$

Lipid droplets were observed to increase with increasing NP concentrations, which could be an indicator or feature of the oxidative stress process (Khatchadourian & Maysinger, 2009; Lee, Homma, Kurahashi, Kang, & Fujii, 2015; Marmorato et al., 2011).

### Cytotoxicity

The results of MTT and NRU assays showed that NiO-NPs decreased the cell metabolic activity after exposure to concentrations ranging from 50 to 500  $\mu\text{g}/\text{mL}$  for 24 h (Figure 7). The dose-dependent reduction of cell metabolic activity and lysosomal functions could be related to an increase in cell death. The  $\text{IC}_{50}$  values were 146.7 and 203.8  $\mu\text{g}/\text{mL}$ .

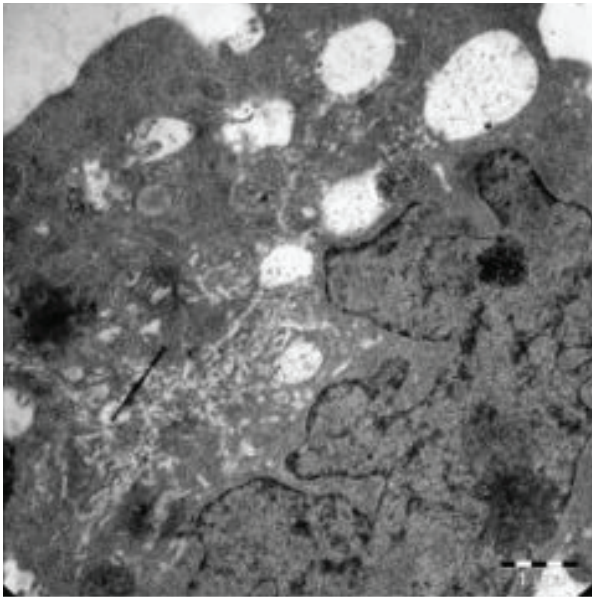
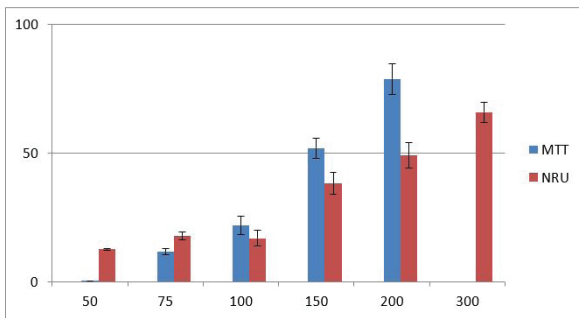


**Figure 6.** TEM observations of HepG2 cells after exposure to NiO-NPs for 24 h.

HepG2 unexposed cell (negative control)



	50	75	100	150	200	300	IC <sub>50</sub>
MTT	0.33	11.63	21.86	51.89	78.74	-	146.7
NRU	12.59	17.8	16.9	38.17	49.06	65.8	203.8

**Figure 7.** NiO-NPs induced cytotoxicity to HepG2 cells.

The cells were exposed to different concentrations (50-300 mg/mL) of NiO-NPs for 24 h. At the end of the exposure time, cytotoxicity parameters were determined with mitochondrial function (MTT) and lysosomal activity (NRU) assays, as described in the Methods section. All experiments were done in triplicates and each assay as repeated four times. Data was expressed as mean±SD.

**Genotoxicity**

The genotoxicity of NiO-NPs was estimated by comet test at concentrations of 15-120 µg/mL (Figure 8). In positive controls (100 µM H<sub>2</sub>O<sub>2</sub>), the tail intensity was 22.6%. The results indicate that NiO-NPs significantly induced DNA damage in all cells (2.5 to 10.6-fold) in a concentration-dependent manner (p≤0.05). At a 120 µg/mL concentration (the highest; the cell deaths were ≤50%) the tail intensities were 22.6%.

**Oxidative damage**

The changes in the widely used oxidative damage parameters (i.e., GSH, MDA, 8-OHdG, and PC levels) were used to estimate the potential of NiO-NPs to induce oxidative damage to HepG2 cells after exposure to 50-150 µg/mL concentrations (Table 2).

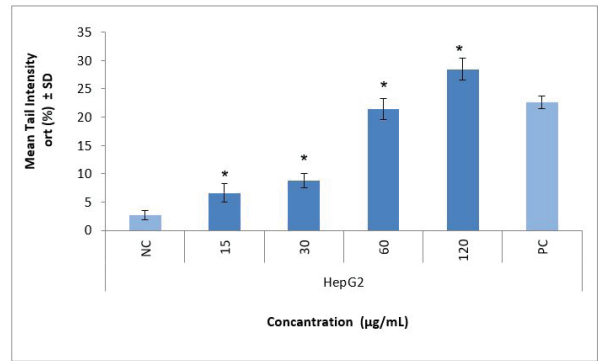


**Figure 8.** NiO-NPs induced genotoxicity to HepG2 cells.

The cells were exposed to different concentrations (15-120 mg/mL) of NiO-NPs for 24 h. At the end of the exposure time, their genotoxicity potential was determined by comet assay, as described in the Methods section. All experiments were done in triplicates and each assay as repeated twice. The results were presented as mean tail intensity (%) with ±SD. NC (PBS) and PC (100 µM H<sub>2</sub>O<sub>2</sub>) mean negative and positive controls, respectively. \*p≤0.05 were selected as the levels of significance by one-way ANOVA Dunnett t-test

The NiO-NPs induced oxidative damage at all exposure concentrations. The levels of MDA were increased significantly (≤1.4-fold). A significant decrease in GSH levels was observed (≤34.2%). While the PC levels increased significantly (≤1.14-fold) at concentrations of 150 µg/mL, the levels were decreased significantly at 75 and 100 µg/mL (≤21.2%). No significant change in 8-OHdG levels was observed. In general, the potential of oxidative stress by NiO-NPs on HepG2 cells was statistically significant compared to the negative control (p≤0.05).

**Table 2. Oxidative stress parameters that demonstrate NiO-NPs induced oxidative damage to HepG2 cells.**

Cells	Exposure concentration (µg/mL)	8-OHdG (µg/g protein)	MDA (µmol/g protein)	GSH (µmol/g protein)	PC (µg/g protein)
HepG2	0	1.13±0.09	0.32±0.06	53.00±1.03	6.61±0.11
	50	1.10±0.15	0.44±0.04*	37.63±1.66*	6.48±0.49
	75	1.04±0.03	0.46±0.08*	39.72±1.98*	5.25±0.19*
	100	1.15±0.49	0.39±0.10*	34.90±2.09*	5.21±0.26*
	150	1.04±0.27	0.41±0.20	41.65±0.84*	7.46±0.20*

The cells were exposed to different concentrations (0-120 mg/mL) of NiO-NPs for 24 h. At the end of the exposure time, 8-OHdG, MDA, GSH and PC levels were determined by ELISA, as described in the Methods section.

**Apoptosis**

Test results indicate that NiO-NPs caused a concentration-dependent increase in the percentage of apoptotic cells (Figure 9). At the highest concentrations of NiO-NPs, equivalent to 75% cell death, the percentage of apoptotic cells was 86.6% whereas the necrotic cells were 13.4%.

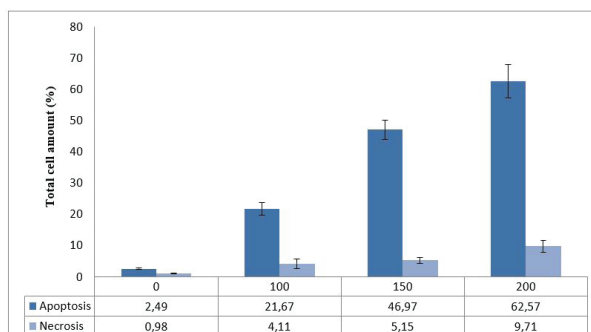


**Figure 9.** NiO-NPs induced apoptosis/necrosis to HepG2 cells.

Cells were exposed to different concentrations of NiO-NPs, equivalent to 25%, 50% and 75% cell death (0-200 mg/mL) for 24 h; At the end of the exposure time, their apoptosis/necrosis inducing potentials were determined by Annexin V-FITC apoptosis detection assay with PI, as described in the Methods section. All experiments were done in triplicates and each assay as repeated twice. The results were expressed as the percent of the total cell amount with  $\pm$ SD. \* $p \leq 0.05$  were selected as the levels of significance by one-way ANOVA Dunnett t-test.

## DISCUSSION

The previous studies showed that NPs could be absorbed through the gastrointestinal tract after accidental ingestion (as air pollution mixed with mucus and saliva) by industry and research laboratory workers or just by drinking and eating contaminated water and food (Ahmad et al., 2013). However, prior *in vitro* studies related to toxicity of NiO-NPs are controversial and mainly focused on the pulmonary system. In this work, it was aimed to evaluate the toxicity profile of NiO-NPs (average size of 15.0 nm) in HepG2 cells, which simulate one of the target organs for NPs after accidental exposure (Sadeghi, Tanwir, & Babadi, 2015; Sahu, Njoroge, Bryce, Yourick, & Sprando, 2014).

According to our results, NiO-NPs cause a dose-dependent decrease in the cellular metabolic activity ( $IC_{50}$ =146.7 – 203.8  $\mu$ g/mL). However, the calculated  $IC_{50}$  values were higher than the values calculated by the previous studies. It is well known that free radicals and oxidative stress outcomes attack lipids, DNA, and proteins (Horie et al., 2011). The previous studies showed that NiO-NPs induce oxidative damage in different cell lines, such as HepG2, human neuroblastoma (SH-SY5Y), human lung carcinoma (A549), human colorectal carcinoma (Caco-2), and human breast epithelial (MCF-7) cells (Abudayyak et al., 2017; 2017b; Ahamed et al., 2011; 2013; Ahmad et al., 2013; Horie et al., 2011; Siddiqui et al., 2012). The previous studies show that the induction of reactive oxygen species (ROS) after exposure to NiO-NPs plays an important role in lung inflammation (Cho et al., 2010; Horie et al., 2012; Jeong, Kim, Seok, & Cho 2016; Ogami et al., 2009). By the same token, Ahamed et al., (2013) reported that NiO-NPs caused cytotoxicity *via* ROS at 25-100  $\mu$ g/mL. In this study, the significant changes in MDA, PC and GSH levels after exposure to 50-150  $\mu$ g/mL concentrations could be an indication for the oxidative damage in the exposed cells.

Ahmed et al., (2013) reported that alteration of lysosomal and mitochondrial functions triggers cell death by apoptosis after exposure to NiO-NPs at 25-100  $\mu$ g/mL. Similarly, the present results show that NiO-NPs altered the cell metabolic activity as assessed by the disruption of lysosome and mitochondrial

functions; the  $IC_{50}$  values 146.7 and 203.8  $\mu$ g/mL by MTT and NRU assays, respectively. In a study that investigated the cytotoxic effect of 24 NPs on human pulmonary cell lines (A549 and THP-1),  $IC_{50}$  values for NiO-NPs were 23.3 and 1613  $\mu$ g/mL in two different labs (Lanone et al., 2009). They emphasized that differences in the sensitivity between cell types and cytotoxicity assays could be possible factors leading to differences in the obtained results and should be carefully considered while estimating NP toxicity.

Ahamed et al., (2013) indicated a significant increase in micronuclei induction in HepG2 cells after exposure to NiO-NPs; they reported up-regulation of mRNA expression levels of apoptotic genes Bax and caspase-3, and a down-regulation in the expression of bcl-2 an anti-apoptotic gene. Caspase-3 enzyme activity was also higher in exposed cells. An increase in caspase-3 enzyme activity was similarly reported by Siddiqui et al., (2012). They also reported a dose-dependent cytotoxicity, oxidative stress, apoptosis, and DNA fragmentation in HEp-2 and MCF-7 cells after exposure to NiO-NPs at 2-100  $\mu$ g/mL. Capasso et al., (2014) indicated NiO-NPs at 20-100  $\mu$ g/mL could be a potent activator of genotoxicity cascade in A549 and BEAS-2B human pulmonary cell lines. They also reported an alteration in the cell cycle of the exposed cells. Similarly, we observed NiO-NPs led to an increase in the percentage of apoptotic cells in a dose-dependent manner in HepG2 cells.

Horie et al., (2009) revealed the uptake of NiO-NPs into human keratinocyte (HaCaT) cells, and the particles were more cytotoxic to HaCaT cells than A549 cells. Duan et al., (2015) investigated the impacts of NiO-NPs on sirtuin 1, a NAD-dependent deacetylase involved in apoptosis in human bronchial epithelial cells (BEAS-2B). They reported an inhibition of the cell viability via the apoptotic process, and indicated that NiO-NP-induced apoptosis could occur *via* tumor protein p53 and bcl-2-associated X protein. As reported by the researchers, we observed NiO-NP-induced DNA damage and apoptotic/necrotic effects on the cells. The degree of apoptosis/necrosis corresponded with the severity of cytotoxicity (Figures 7 and 9). The apoptosis stage observed in HepG2 cells could depend on the damage of mitochondrial functions.

In conclusion, NiO-NPs are one of the widespread metal-based nanoparticles. The accidentally up taken NPs could attain the liver as one of the target organs. The previous studies emphasize the possible toxic effects of NiO-NPs on different target organs and cell lines. HepG2 was used previously to evaluate the toxicity of NiO-NPs. However, as different labs, the different methods and differently synthesized NPs could give different results, we have tried in this work to re-evaluate the same NPs using the same cell line but with different methods and assays. The results confirm the previous data; the DNA damage, apoptosis, and oxidative stress effects of NiO-NPs should attract attention. Further *in vivo* and *in vitro* studies using previously tested and new cell lines and animal models with different assays and protocols should be carried out to illuminate the safety associated with NiO-NPs and other NPs applications. Besides that, the supporting studies are needed to fully understand the mechanism of NiO-NP toxicity.

**Peer-review:** Externally peer-reviewed.

**Author contributions:** Conception/Design of Study- M.A., G.Ö.; Data Acquisition- M.A., G.Ö.; Data Analysis/Interpretation- M.A., G.Ö.,E.E.G.; Drafting Manuscript- M.A., G.Ö.,E.E.G.; Critical Revision of Manuscript- M.A., G.Ö.; Final Approval and Accountability- M.A., G.Ö.,E.E.G.

**Conflict of Interest:** The authors have no conflict of interest to declare.

**Financial Disclosure:** This work was supported by the Research Fund of Istanbul University (Project No: 37785).

## REFERENCES

- Abudayyak, M., Guzel, E., & Özhan, G. (2017a). Nickel oxide nanoparticles induce oxidative DNA damage and apoptosis in kidney cell line (NRK-52E). *Biological Trace Element Research*, 178(1), 98-104. <https://doi.org/10.1007/s12011016-0892-z>.
- Abudayyak, M., Guzel, E., & Özhan, G. (2017b). Nickel oxide nanoparticles are highly toxic to SH-SY5Y neuronal cells. *Neurochemistry International*, 108, 7-14. <https://doi.org/10.1016/j.neuint.2017.01.017>.
- Ahamed, M. (2011). Toxic response of nickel nanoparticles in human lung epithelial A549 cells. *Toxicology in vitro*, 25(4), 930-936. <https://doi.org/10.1016/j.tiv.2011.02.015>.
- Ahamed, M., Akhtar, M.J., Siddiqui, M.A., Ahmad, J., Musarrat, J., Al-Khedhairi, A.A. ... Alrokayan, S.A. (2011). Oxidative stress mediated apoptosis induced by nickel ferrite nanoparticles in cultured A549 cells. *Toxicology*, 283(2-3), 101-108. <https://doi.org/10.1016/j.tox.2011.02.010>.
- Ahamed, M., Ali, D., Alhadlaq, H.A., & Akhtar, M.J. (2013). Nickel oxide nanoparticles exert cytotoxicity via oxidative stress and induce apoptotic response in human liver cells (HepG2). *Chemosphere*, 93(10), 2514-2522. <https://doi.org/10.1016/j.chemosphere.2013.09.047>.
- Ahmad, J., Alhadlaq, H.A., Siddiqui, M.A., Saquib, Q., Al-Khedhairi, A.A., Musarrat, J., & Ahamed, M. (2013). Concentration-dependent induction of reactive oxygen species, cell cycle arrest and apoptosis in human liver cells after nickel nanoparticles exposure. *Environmental Toxicology*, 30, 137-148. <https://doi.org/10.1002/tox.21879>.
- Arora, S., Rajwade, J.M., & Paknikar, K.M. (2012). Nanotoxicology and in vitro studies: the need of the hour. *Toxicology and Applied Pharmacology*, 258(2), 151-165. <https://doi.org/10.1016/j.taap.2011.11.010>.
- Barillet, S., Simon-Deckers, A., Herlin-Boime, N., Mayne-L'Hermite, M., Reynaud, C., Cassio, D., & Carrière, M. (2010). Toxicological consequences of TiO<sub>2</sub>, SiC nanoparticles and multi-walled carbon nanotubes exposure in several mammalian cell types: an in vitro study. *Journal of Nanoparticle Research*, 12(1), 61-73. <https://doi.org/10.1007/s11051-009-9694-y>.
- Boverhof, D.R., & Raymond M.D. (2010). Nanomaterial characterization: considerations and needs for hazard assessment and safety evaluation. *Analytical and Bioanalytical Chemistry*, 396(3), 953-961. <https://doi.org/10.1007/s00216-009-3103-3>.
- Bradford, M.M. (1976). A rapid and sensitive method for the quantitation of microgram quantities of protein utilizing the principle of protein-dye binding. *Analytical Biochemistry*, 7, 248-254. <https://doi.org/10.1006/abio.1976.999>.
- Brand, R.M., Hannah, T.L., Mueller, C., Cetin, Y., & Hamel, F.G. (2000). A novel system to study the impact of epithelial barrier on cellular metabolism. *Annals of Biomedical Engineering*, 28, 1210-1217. <https://doi.org/10.1114/1.1318926>.
- Brooking, J., Davis, S.S., & Illum, L. (2001). Transport of nanoparticles across the rat nasal mucosa. *Journal of Drug Targeting*, 9, 267-279. <https://doi.org/10.3109/10611860108997935>.
- Capasso, L., Marina, C., & Maurizio, G. (2014). Nickel oxide nanoparticles induce inflammation and genotoxic effect in lung epithelial cells. *Toxicology Letters*, 226(1), 28-34. <https://doi.org/10.1016/j.toxlet.2014.01.040>.
- Chen, X., Wang, Z., Zhou, J., Fu, X., Liang, J., Qiu, Y., & Huang, Z. (2014). Renal interstitial fibrosis induced by high-dose mesoporous silica nanoparticles via the NF-KB signaling pathway. *International Journal of Nanomedicine*, 10, 1-22. <https://doi.org/10.2147/IJN.S73538>.
- Cho, W.S., Duffin, R., Poland, C.A., Howie, S.E., MacNee, W., Bradley, M. ... Donaldson, K. (2010). Metal oxide nanoparticles induce unique inflammatory footprints in the lung: important implications for nanoparticle testing. *Environmental Health Perspectives*, 118(12), 1699-1706. <https://doi.org/10.1289/ehp.1002201>.
- Collins, A.R. (2004). The comet assay for DNA damage and repair: principles, applications, and limitations. *Applied Biochemistry and Biotechnology - Part B Molecular Biotechnology*, 26(3), 249-261. <https://doi.org/10.1385/MB:26:3:249>.
- Dhawan, A., & Sharma, V. (2010). Toxicity assessment of nanomaterials: methods and challenges. *Analytical and Bioanalytical Chemistry* 398(2), 589-605. <https://doi.org/10.1007/s00216-010-3996-x>.
- Duan, W.X., He, M.D., Mao, L., Qian, F.H., Li, Y.M., Pi, H.F. ... Zhou, Z. (2015). NiO nanoparticles induce apoptosis through repressing SIRT1 in human bronchial epithelial cells. *Toxicology and Applied Pharmacology*, 286(2), 80-91. <https://doi.org/10.1016/j.taap.2015.03.024>.
- Dunnick, J.K., Benson, J.M., Hobbs, C.H., Hahn, F.F., Cheng, Y.S., & Eidson, A.F. (1988). Comparative toxicity of nickel oxide, nickel sulphate hexahydrate, and nickel subsulfide after 12 days of inhalation exposure to F344/N rats and B6C3F1 mice. *Toxicology*, 50, 145-156. [https://doi.org/10.1016/0300-483X\(88\)90087-X](https://doi.org/10.1016/0300-483X(88)90087-X).
- Horev-Azaria, L., Kirkpatrick, C.J., Korenstein, R., Marche, P.N., Maimon, O., Ponti, J. ... Villiers, C. (2011). Predictive toxicology of cobalt nanoparticles and ions: comparative in vitro study of different cellular models using methods of knowledge discovery from data. *Journal of Toxicological Sciences*, 122, 489-501. <https://doi.org/10.1093/toxsci/kfr124>.
- Horie, M., Fukui, H., Nishio, K., Endoh, S., Kato, H., Fujita, K., Miyachi, A. ... Iwahashi, H. (2011). Evaluation of acute oxidative stress induced by NiO nanoparticles in vivo and in vitro. *Journal of Occupational Health*, 53, 64-74. <https://doi.org/10.1539/joh.110121>.
- Horie, M., Fukui, H., Endoh, S., Maru, J., Miyachi, A., Shichiri, M. ... Iwahashi, H. (2012). Comparison of acute oxidative stress on rat lung induced by nano and fine-scale, soluble and insoluble metal oxide particles: NiO and TiO<sub>2</sub>. *Inhalation Toxicology*, 24(7), 391-400. <https://doi.org/10.3109/08958378.2012.682321>.
- Horie, M., Nishio, K., Fujita, K., Kato, H., Nakamura, A., Kinugasa, S. ... Nakanishi, J. (2009). Ultrafine NiO particles induce cytotoxicity in vitro by cellular uptake and subsequent Ni(II) release. *Chemical Research in Toxicology*, 22(8), 1415-1426. <https://doi.org/10.1021/tx900171n>.
- International Agency for Research on Cancer (IARC). (1990). Nickel compounds group 1, IARC monographs on the evaluation of carcinogenic risks to human's chromium, nickel and welding. *IARC* 49, 257-411.
- Jeong, J., Kim, J., Seok, S.H., & Cho, W.S. (2016). Indium oxide (In<sub>2</sub>O<sub>3</sub>) nanoparticles induce progressive lung injury distinct from lung injuries by copper oxide (CuO) and nickel oxide (NiO) nanoparticles. *Archives of Toxicology*, 90(4), 817-828. <https://doi.org/10.1007/s00204-015-1493-x>.

- Kang, G.S., Gillespie, P.A., Gunnison, A., Rengifo, H., Koberstein, J., & Chen, L.C. (2011). Comparative pulmonary toxicity of inhaled nickel nanoparticles; role of deposited dose and solubility. *Inhalation Toxicology*, 23(2), 95-103. <https://doi.org/10.3109/08958378.2010.543440>.
- Khatchadourian, A., & Maysinger, D. (2009). Lipid droplets: their role in nanoparticle-induced oxidative stress. *Molecular Pharmaceutics*, 6(4), 1125-1137. <https://doi.org/10.1021/mp900098p>.
- Kim, Y.J., Yu, M., Park, H.O., & Yang, S.I. (2010). Comparative study of cytotoxicity, oxidative stress and genotoxicity induced by silica nanomaterials in human neuronal cell line. *Molecular and Cellular Toxicology*, 6(4), 337-344. <https://doi.org/10.1007/s13273-010-0045-y>.
- Lanone, S., Rogerieux, F., Geys, J., Dupont, A., Maillot-Marechal, E., Boczkowski, J. ... Hoet, P. (2009). Comparative toxicity of 24 manufactured nanoparticles in human alveolar epithelial and macrophage cell lines. *Particle and Fibre Toxicology*, 6, 1-12. <https://doi.org/10.1186/1743-8977-6-14>.
- Lee, J., Homma, T., Kurahashi, T., Kang, E.S., & Fujii, J. (2015). Oxidative stress triggers lipid droplet accumulation in primary cultured hepatocytes by activating fatty acid synthesis. *Biochemical and Biophysical Research Communications*, 464(1), 229-235. <https://doi.org/10.1016/j.bbrc.2015.06.121>.
- Marmorato, P., Ceccone, G., Gianoncelli, A., Pascolo, L., Ponti, J., Rossi, F. ... Kiskinova, M. (2011). Cellular distribution and degradation of cobalt ferrite nanoparticles in balb/3T3 mouse fibroblasts. *Toxicology Letters*, 207(2), 128-136. <https://doi.org/10.1016/j.toxlet.2011.08.026>.
- Martin, K.R., Failla, M.L., & Smith, J.C. (1997). Differential susceptibility of Caco-2 and HepG2 human cell lines to oxidative stress. *Journal of the Elisha Mitchell Scientific Society*, 113(4), 149-162. <https://www.jstor.org/stable/44706114>.
- Morimoto, Y., Ogami, A., Todoroki, M., Yamamoto, M., Murakami, M., Hirohashi, M. ... Tanaka, I. (2010). Expression of inflammation-related cytokines following intratracheal instillation of nickel oxide nanoparticles. *Nanotoxicology*, 4(2), 161-176. <https://doi.org/10.3109/17435390903518479>.
- Morimoto, Y., Hirohashi, M., Ogami, A., Oyabu, T., Myojo, T., Hashib, M. ... Tanaka, I. (2011). Pulmonary toxicity following an intratracheal instillation of nickel oxide nanoparticle agglomerates. *Journal of Occupational Health*, 53(4), 293-295. <https://doi.org/10.1539/joh.11-0034-BR>.
- Napierska, D., Thomassen, L.C., Lison, D., Martens, J.A., & Hoet, P.H. (2010). The nanosilica hazard: another variable entity. *Particle and Fibre Toxicology*, 7(1), 39. <https://doi.org/10.1186/1743-8977-7-39>.
- Nishi, K., Morimoto, Y., Ogami, A., Murakami, M., Myojo, T., Oyabu, T., Kadoya, C. ... Tanaka, I. (2009). Expression of cytokine-induced neutrophil chemoattractant in rat lungs by intratracheal instillation of nickel oxide nanoparticles. *Inhalation Toxicology*, 21, 1030-1039. <https://doi.org/10.1080/08958370802716722>.
- O'Brien, P.J., Irwin, W., Diaz, D., Howard-Cofield, E., Krejsa, C.M., Slaughter, M.R., Gao, B. ... Hougham, C. (2006). High concordance of drug-induced human hepatotoxicity with in vitro cytotoxicity measured in a novel cell-based model using high content screening. *Archives of Toxicology*, 80, 580-604. <https://doi.org/10.1007/s00204-006-0091-3>.
- Oberdorster, G. (2001). Pulmonary effects of inhaled ultrafine particles. *International Archives of Occupational and Environmental Health*, 74, 1-8. <https://doi.org/10.1007/s004200000185>.
- Oberdorster, G., Oberdorster, E., & Oberdorster, J. (2005). Nanotoxicology: An emerging discipline evolving from studies of ultrafine particles. *Environmental Health Perspectives* 113, 823-839. <https://doi.org/10.1289/ehp.7339>.
- Ogami, A., Morimoto, Y., Myojo, T., Oyabu, T., Murakami, M., Todoroki, M. ... Tanaka, I. (2009). Pathological features of different sizes of nickel oxide following intratracheal instillation in rats. *Inhalation Toxicology*, 21(10), 812-818. <https://doi.org/10.1080/08958370802499022>.
- Oyabu, T., Ogami, A., Morimoto, Y., Shimada, M., Lenggono, W., Okuyama, K., & Tanaka, I. (2007). Biopersistence of inhaled nickel oxide nanoparticles in rat lung. *Inhalation Toxicology*, 19(1), 55-58. <https://doi.org/10.1080/08958370701492995>.
- Repetto, G., del Peso, A., & Zurita, J.L. (2008). Neutral red uptake assay for the estimation of cell viability/cytotoxicity. *Nature Protocols*, 3(7), 1125-1131. <https://doi.org/10.1038/nprot.2008.75>.
- Sadeghi, L., Tanwir, F., & Babadi, V.Y. (2015). In vitro toxicity of iron oxide nanoparticle: oxidative damages on HepG2 cells. *Experimental and Toxicologic Pathology*, 67, 197-203. <https://doi.org/10.1016/j.etp.2014.11.010>.
- Sahu, S., Njoroge, J., Bryce, S.M., Yourick, J.J., & Sprando, R.L. (2014). Comparative genotoxicity of nanosilver in human liver HepG2 and colon Caco2 cells evaluated by a flow cytometric in vitro micronucleus assay. *Journal of Applied Toxicology*, 34, 1226-1234. <https://doi.org/10.1002/jat.3065>.
- Schrand, A.M., Rahman, M.F., Hussain, S.M., Schlager, J.J., Smith, D.A., & Syed, A.F. (2010). Metal-based nanoparticles and their toxicity assessment. *Wiley Interdisciplinary Reviews: Nanomedicine and Nanobiotechnology*, 2(5), 544-568. <https://doi.org/10.1002/wnan.103>.
- Siddiqui, M.A., Ahamed, M., Ahmad, J., Majeed Khan M.A., Musarrat, J. Al-Khedhairi, A.A., & Alrokayan, S.A. (2012). Nickel oxide nanoparticles induce cytotoxicity, oxidative stress and apoptosis in cultured human cells that is abrogated by the dietary antioxidant curcumin. *Food and Chemical Toxicology*, 50(3-4), 641-647. <https://doi.org/10.1016/j.fct.2012.01.017>.
- Speit, G., & Hartmann, A. (1999). The comet assay (single-cell gel test). A sensitive genotoxicity test for the detection of DNA damage and repair. *Methods in Molecular Biology* 113, 203-212. <https://doi.org/10.1385/1-59259-675-4:203>.
- Van Meerloo, J., Kaspers, G.J., & Cloos, J. (2011). Cell sensitivity assays: the MTT assay. *Methods in Molecular Biology* 731, 237-245. [https://doi.org/10.1007/978-1-61779-080-5\\_20](https://doi.org/10.1007/978-1-61779-080-5_20).
- Walczyk, D., Bombelli, F.B., Monopoli, M.P., Lynch, I., & Dawson, K.A. (2010). What the cell "Sees" in bionanoscience. *Journal of the American Chemical Society* 132(16), 5761-5768. <https://doi.org/10.1021/ja910675v>.
- Zhang, H., Ji, Z., Xia, T., Low-Kam, C., Liu, R., Pokhrel, S. ... Nel, A.E. (2012). Use of metal oxide nanoparticle band gap to develop a predictive paradigm for oxidative stress and acute pulmonary inflammation. *ACS Nano* 6, 4349-4368. <https://doi.org/10.1021/nn3010087>.